Journal of Magnetism and Magnetic Materials 464 (2018) 44–49

Contents lists available at ScienceDirect

Journal of Magnetism and Magnetic Materials

journal homepage: www.elsevier.com/locate/jmmm

Research articles

Colossal magnetostriction and electrostriction of bismuth-substituted neodymium iron garnet films

S.S. Aplesnin[a,b,*], A.N. Masyugin[a], M.N. Sitnicov[a], U.I. Rybina[a], Takayuki Ishibashi[c]

[a] Reshetnev Siberian State University of Science and Technology, Krasnoyarsk 662850, Russian Federation
[b] Kirensky Institute of Physics of SB RAS, Krasnoyarsk 660036, Russian Federation
[c] Department of Materials Science and Technology, Nagaoka University of Technology, Nagaoka, Niigata 940-2188, Japan

ARTICLE INFO

Keywords:
Thermal expansion
Magnetostriction
Electrostriction

ABSTRACT

Electro- and magnetostriction mechanisms and temperature behavior of the length of bismuth-substituted neodymium iron garnet films on glass and gallium gadolinium garnet have been investigated. Electric- and magnetic-field and temperature dependences of the electro- and magnetostriction constants have been determined. It has been established that the magnetostriction constant changes its sign upon temperature variation. The experimental data are explained using a model of dipole glass with the magnetoelectric and magnetoelastic interaction.

1. Introduction

Bi-substituted rare-earth iron garnets have been used as optical isolators and other magnetooptical (MO) devices since they exhibit a large MO effect in the visible light region. Bi-substituted garnets are expected to be used as spatial light modulators, waveguide-type isolators, and MO indicators [1–3]. The MO effects are enhanced with increasing Bi substitution due to the change in the spin-orbit interaction contributed to by the 6p orbital of Bi [4–6] for example, Faraday rotation reaches 25°/μm around 530 nm in a fully Bi-substituted rare-earth iron garnet, $Bi_3Fe_5O_{12}$ (BIG). Therefore, garnets substituted with a large amount of Bi have been attracting attention as materials for MO applications [7–10].

The magnetic and structural characteristics of thin films depend on a substrate used. In particular, the lattice constant of the $Nd_xBi_{1-x}Fe_{5-y}Ga_yO_{12}$ film in the (1 1 1) direction is smaller than that in the (1 0 0) direction by 0.2% [11]. In bulk neodymium-substituted yttrium iron garnet samples, the first (K1) and second (K2) anisotropy constants are comparable; below 80 K, the constant K2 is larger than the constant K1 [12]. The magnetostriction constants are negative and their absolute value in $Yt_{2.5}Nd_{0.5}Fe_5O_{12}$ slightly grows with a decrease in temperature down to 77 K [13]. The magnetostriction of these compounds is determined by the single-ion character of a rare-earth element caused by the paraprocess.

The bismuth ferrite films exhibit the magnetoelectric properties [14], which originate from the electric polarization [15,16] and magnetic order [17,18]. The authors of [16] observed the magnetic-field-driven electric polarization of domain walls in the 10-μm-thick $(Bi-Lu)_3(FeGa)_5O_{12}$ films grown by liquid-phase epitaxy on the (2 1 0) $Gd_3Ga_5O_{12}$ substrate. In the films grown on the (1 1 1) substrates, the electric polarization is not observed. These effects are related to the nonuniformity of the magnetoelectric interaction and electric-field-driven magnetic anisotropy variation [19]. The linear magnetoelectric effect was found in the 90-nm-thick bismuth ferrite films on (0 0 1) $Y_3Al_5O_{12}$ garnet (YAG) by a resonant technique with the electric field modulation [20]. The giant linear magnetoelectric effect in garnet ferrite films is revealed by the polarimetric method in magnetic fields up to 10 kOe [21]. The linear magnetoelectric interaction was attributed to the strong spin-orbit coupling and occurrence of a local magnetic inhomogeneity.

Multiferroic materials are characterized by the strong interrelation of the magnetic and electric subsystems, which is implemented in single-phase ferromagnetic materials by means of the spin-lattice and electron-lattice interactions. Study of single-phase materials with the high magnetostriction and large piezoelectric modulus in multiferroics is important for deeper understanding of electromagnetic phenomena in solids and creation of the new generation of solid-state electronic devices.

Yttrium iron garnet has a cubic symmetry with the inversion center [22] and undergoes a structural transition with the triclinic lattice distortion below 130 K [23]. The electric polarization can originate from the structural strain, which breaks the inversion center by means of epitaxial stresses of the film on a substrate or cation substitution over dodecahedral sites, as well as from the surface electronic states or

* Corresponding author at: Reshetnev Siberian State University of Science and Technology, Krasnoyarsk 662850, Russian Federation.
E-mail address: apl@iph.krasn.ru (S.S. Aplesnin).

https://doi.org/10.1016/j.jmmm.2018.05.038
Received 27 March 2018; Received in revised form 15 May 2018; Accepted 15 May 2018
Available online 16 May 2018
0304-8853/ © 2018 Elsevier B.V. All rights reserved.

magnetic domain structure induced by demagnetizing fields. The latter can be excluded when the measurements are performed in the external magnetic field stronger than the saturation field by an order of magnitude. The effect of epitaxial stresses can be elucidated by using two types of substrates and different substitutes (neodymium and gallium). The role of elastic stresses can be established from the magneto- and electrostriction data.

The aim of this study was to clarify a mechanism of magneto- and electrostriction and thermal expansion of the bismuth–neodymium iron garnet films deposited onto glass and garnet substrates.

2. Results and discussion

2.1. Thermal expansion of the films

We investigated the films of two types: $Nd_1Bi_2Fe_5O_{12}$(450 nm)/ $Nd_2Bi_1Fe_4Ga_1O_{12}$(90 nm) films deposited onto glass and $Nd_{0.5}Bi_{2.5}Fe_5O_{12}$(450 nm) films on a (1 1 1) single-crystal $Gd_3Ga_5O_{12}$ garnet (GGG) substrate. The films were grown epitaxially. Using the bilayer film enable to switch the direction of the magnetic moment and modulate the value of the Faraday angle of rotation in a magnetic field.

The relative change in the length of films was determined with ZFLA-3-11 strain gauges with a resistance of 140 Ω. One strain gauge was located on the film, the other on the substrate. The difference between resistances of two gauges (on the film (R_f) and on the substrate (R_s)) $\delta L = (R_f - R_s)/R_s = (L_f - L_s)/L_s$ was measured. The magnetostriction constant was determined from the variation in the strain gauge resistance $\lambda = (R(H) - R(0))/R(0) = (L(H) - L(0))/L(0)$ in a magnetic field. Fig. 1a shows the relative change in the length of a film deposited onto glass upon temperature variation. The thermal expansion coefficient d(δL)/dT of the film has several anomalies; in particular, the relative change in the film length sharply drops at T = 194, 294, and 445 K and the film is strongly expanded at T = 358 and 416 K. Above room temperature, the film is expanded upon heating and attains its maximum length at the Curie temperature. The change in the d(δL)/dT sign around room temperature is related to the dipole glass formation. The maximum expansion of the film in the vicinity of the transition temperature can be caused by the iron ion spin fluctuations, which lead to the expansion of the film due to the magnetoelastic interaction.

The temperature dependence of the thermal expansion of the $Nd_{0.5}Bi_{2.5}Fe_5O_{12}$ film on the iron garnet substrate is qualitatively different (Fig. 1b). Above 160 K, the thermal expansion of the film sharply increases and exhibits a small maximum at 298 K. The interaction between the film and GGG substrate is stronger than in the case of amorphous glass. Epitaxial strain, followed by fast lattice relaxation and relaxed for thicknesses above a few tens of nanometers [1]. On the interface the deformation exists within the 20–30 lattice constants. Part of the volume of the film changes with a temperature similar to the substrate, and the expansion of the rest of the film is due to various types of interactions in the film. Thus, the substrate is responsible for the thermal expansion of the film.

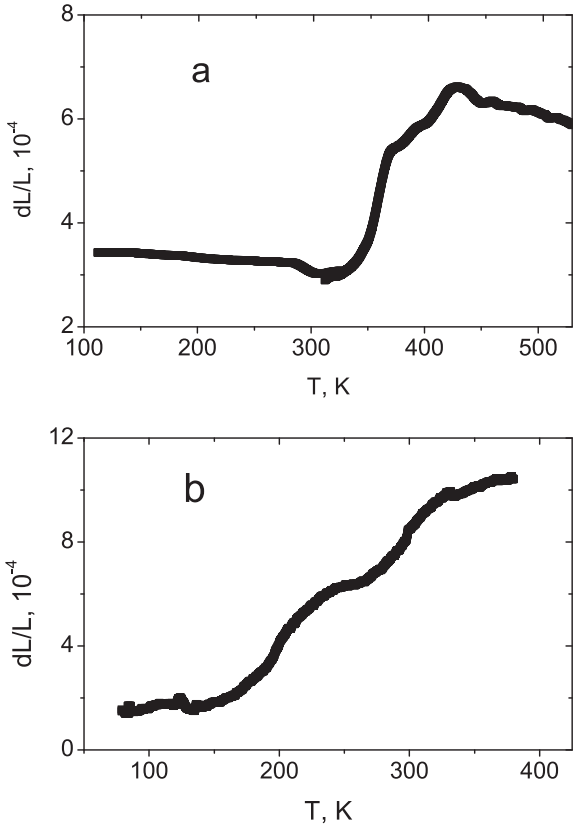

Fig. 1. Relative change in the length of $Nd_1Bi_2Fe_5O_{12}$ (450 nm) / $Nd_2Bi_1Fe_4Ga_1O_{12}$ (90 nm) films on a glass substrate (a) and $Nd_{0.5}Bi_{2.5}Fe_5O_{12}$ (450 nm) on a $Gd_3Ga_5O_{12}$ single crystal substrate (GGG) as a function of temperature.

2.2. Magneto- and electrostriction of the films

Fig. 2 presents the magnetostriction constant of the film deposited onto glass as a function of the magnetic field applied perpendicular to the film. Around room temperature, one can observe the nonlinear λ(H) dependence. In a magnetic field of H = 12 kOe, the magnetostriction

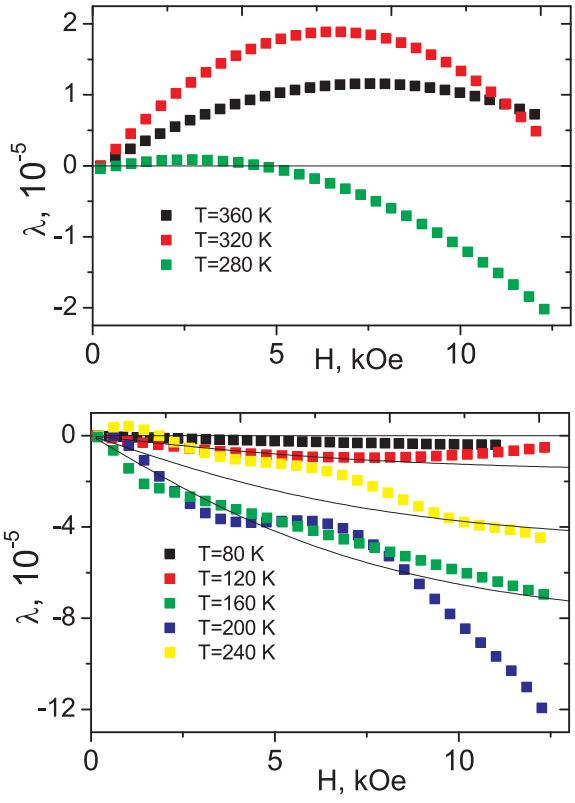

Fig. 2. The magnetostriction constant $\lambda = (L(H) - L(0))/L(0)$ of the film $Nd_1Bi_2Fe_5O_{12}$(450 nm)/$Nd_2Bi_1Fe_4Ga_1O_{12}$(90 nm) on glass substrates at a fixed temperature as a function of the magnetic field. Theoretical values of λ, calculated from the expression (9) (solid lines).

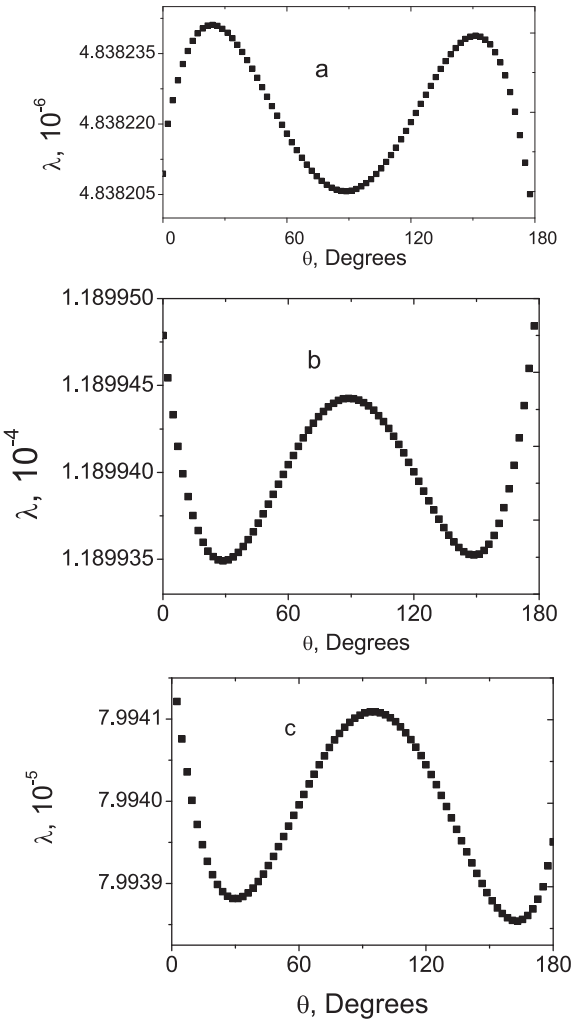

Fig. 3. The magnetostriction constant of the film $Nd_1Bi_2Fe_5O_{12}$(450 nm)/$Nd_2Bi_1Fe_4Ga_1O_{12}$(90 nm) on a glass substrate from the angle between the normal of the film and the magnetic field H = 12 kOe at T = 320 K (a), 200 K (b), 160 K (c).

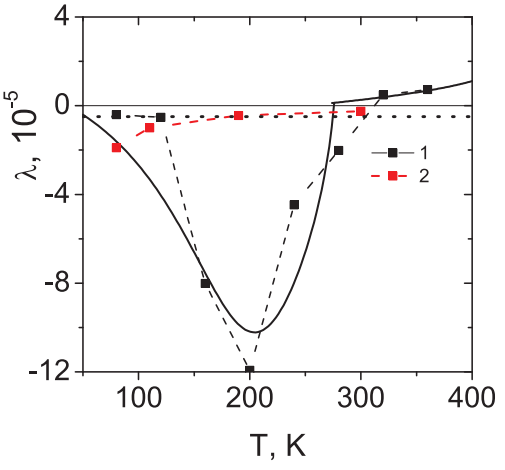

Fig. 4. The temperature dependence of magnetostriction constant of the film $Nd_1Bi_2Fe_5O_{12}$(450 nm)/$Nd_2Bi_1Fe_4Ga_1O_{12}$(90 nm) on a glass substrate (1), ferrite garnet $Y_{2.5}Nd_{0.5}Fe_5O_{12}$ (2) [13]. and theory (9) (solid line).

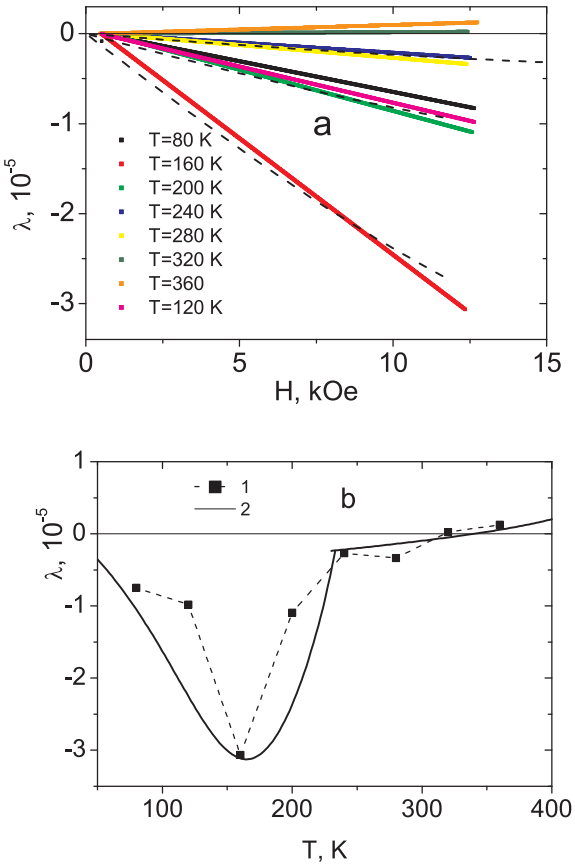

Fig. 5. Magnetostriction constants of film $Nd_{0.5}Bi_{2.5}Fe_5O_{12}$ on garnet at fixed temperatures as a function of magnetic field (a) and temperature: 1- experiment, 2-theory (9) in a magnetic field of H = 12 kOe (b).

constant changes its sign below 310 K. The maximum film compression was observed at a temperature of 200 K. At low temperatures, the magnetostriction constant decreases by an order of magnitude. There is the slight magnetostriction anisotropy (Fig. 3). Upon rotation of the film relative to the magnetic field, the film elongation is maximum at an angle of 24°. Below 280 K, the minimum and maximum of magnetostriction is attained at 30° and in the direction perpendicular to the film. The temperature dependence of the magnetostriction constant in a magnetic field of 12 kOe is shown in Fig. 4.

The film on the GGG substrate is linearly expanded in a magnetic field at T > 300 K and compressed below room temperature. The field dependence of magnetostriction is presented in Fig. 5a. As the temperature decreases, the magnetostriction changes its sign, passes through the minimum at T = 160 K, and, as in the film on glass, remains almost temperature-independent upon further cooling (Fig. 5b). The magnetostriction constant almost does not change with the magnetic field orientation (the magnetostriction is bulk).

The relative change in the lengths of the $Nd_1Bi_2Fe_5O_{12}$(450 nm)/$Nd_2Bi_1Fe_4Ga_1O_{12}$(90 nm) film on the glass substrate was measured in electric fields of up to 400 V/cm (Fig. 6). The film is slightly expanded in the external electric field at T = 80 K. Above T = 120 K, the film is linearly compressed; the maximum compression is attained in fields of 300–400 V/cm at T > 200 K. This dependence is similar to the dependence of a superparamagnetics in a magnetic field. Above room temperature, there are two competing mechanisms, one of which is related to the film compression and the other, to the film expansion. In this temperature range, the magnetostriction changes its sign. The film

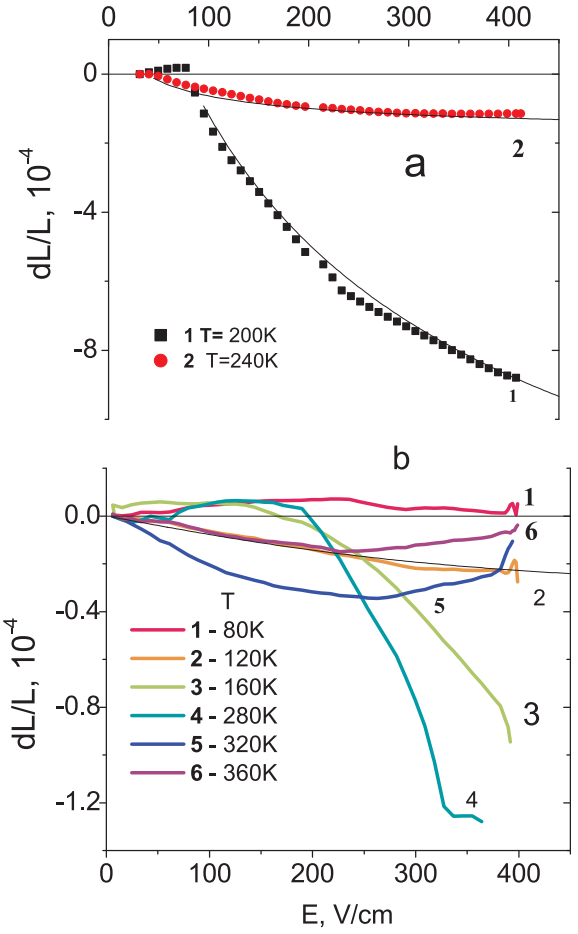

Fig. 6. Relative change in the length of $Nd_1Bi_2Fe_5O_{12}$(450 nm)/$Nd_2Bi_1Fe_4Ga_1O_{12}$(90 nm) film on glass at fixed temperatures as a function of electric field at T = 200 K (1), 240 K (2) (a): T = 80 K (1), 120 K (2), 280 K(3), 320K (5), 360 K (6) (б). The solid line represents a fitting function $dL/L = A_1 \Delta P/\Delta E - A_2 E^n$.

strain is independent of the electric field sign. The electrostriction increases in its absolute value with increasing temperature, passes through its maximum at 200 K, and decreases with a further increase in temperature to 360 K.

3. Model

The concentration dependence of magnetostriction of the neodymium-substituted yttrium iron garnets is linear and explained in the framework of a single-ion model [13]. The temperature dependence of magnetostriction of bismuth iron garnet cannot be described by a single-ion model and requires the polar character of the covalent bond to be taken into account. In bismuth iron garnet, the magnetic moment decreases by 0.6 μ_B per $Bi_3Fe_5O_{12}$ formula unit relative to a Fe^{3+} ion magnetic moment of 5 μ_B [10]. According to the nuclear magnetic resonance (NMR) data, the internal field on the Bi^{3+} core is 60 kOe [24]; its origin remains unclear. The films with a thickness of 100–300 nm exhibit the easy-plane magnetic anisotropy Ha/He ~ 10^{-2} and their magnetization is temperature-independent up to 120 K [22]. The magnetic moment direction in the $Bi_3Fe_5O_{12}$ film depends on a substrate used and amounts to 34° on the $Sm_3[(ScGa)sO]_2$ substrate [10]. The substrate induces the anisotropy by means of elastic stresses at the interface.

In addition, elastic stresses can be induced in a film by the electric field. The maximum film compression in magnetic and electric fields is observed at the same temperature. This is indicative of the interrelation of magnetic and dielectric properties. The magnetoelectric coupling causes the magnetic-field dependence of polarization. There are several probable polarization mechanisms, specifically, a slight deviation from the central symmetry caused by the epitaxial straining or cation substitution in dodecahedral lattice sites, the presence of long pairs of bismuth ions and strong spin-orbit coupling, and domain structure of the sample. The latter can be excluded when the measurements are performed in the magnetic fields corresponding to the saturation magnetization. The magnetoelectric effect can be explained, in particular, by a slight lattice strain caused by the epitaxial growth of a film on the substrate mismatched with the lattice. The garnet cubic symmetry lowering can give rise to the magnetoelectric effect. The change in the distance between magnetically active ions affects the degree of overlap of the wave functions of magnetic ions and oxygen anions. The bismuth ion has an unshared electron pair $6s^2$, which is involved in hybridization of the wave functions with oxygen, changes the indirect exchange coupling between iron ion spins, and leads to the lattice straining. There are broken oxygen bonds on the film surface and anion defects near it. This can also lead to the local electric polarization, since the dipole moments are randomly distributed over the lattice and form dipole glass. An anion vacancy is compensated by an electron from the iron ion sublattice. The valence exchange between di- and trivalent iron ions affects the magnetostriction value.

The magnetoelectric interaction can be caused by the spin-orbit coupling. The calculation of the $Bi_3Fe_5O_{12}$ electronic structure using the electron density functional theory with take into account of relativistic corrections showed the enhancement of the spin-orbit coupling due to the Bi 6p hybridization with oxygen and iron ions. Splitting of the oxygen 2p valence band, iron 3d valence band, and conduction band is larger than in $Y_3Fe_5O_{12}$ by 7, 4, and 13 meV, respectively [25]. The experimental splitting of the t_{2g} states caused by the spin-orbit coupling is 39.4 mV [26]. The calculated and measured gaps in the electron excitation spectrum differ by a factor of 3. Therefore, we may assume the valence-band splitting caused by the spin-orbit coupling to be 20 mV and the conduction-band splitting to be 40 mV. The electronic structure rearrangement will lead to the change in the g factor.

Generally, the bulk magnetostriction depends on the change in the exchange coupling parameters with the distance ($dHex/d\varepsilon$), the change in the anisotropy constant with the strain ($dD/d\varepsilon$), and the change in the g-factor parameter ($dg/d\varepsilon$). In rare-earth iron garnets, the single-ion mechanism prevails, which is related to the paraprocess resulting from the weak interaction between the rare-earth-element sublattice and iron ions. The strain is determined as ε = BM H_{ef}/Δ, where B is the modulus of elasticity, Δ is the energy between the ground and excited states (Δ = 2000 cm^{-1} for Nd^{+3}), M is the magnetization of a neodymium ion ($M = gJ\ (J + 1)\mu_B\ B_J(x)$, $B_J(x)$ is the Brillouin function), and H_{ef} is the effective exchange field induced by iron ion spins [27]. For the paraprocess, we have $\varepsilon = B\ (g\ \mu_B)^2\ J\ (J + 1)\ H_{ef}{}^2/(3\Delta k_B T)$ and the magnetostriction constant is

$$\lambda_a = d\varepsilon/dH = B(g\ \mu_B)^2 J\ (J + 1) 2H_{ef}\ (dH_{ef}/dH)/(3\Delta k_B T) \quad (1)$$

This dependence qualitatively describes the experimental data obtained for $Nd_{0.5}Yt_{2.5}Fe_5O_{12}$ [13] with the parameters B = 100 cm^{-1}, H_{ef} = 2 mV, and dH_{ef}/dH = 0.01 and does not describe the temperature dependence of magnetostriction of the bismuth iron garnet films.

The electrostriction of the films is mainly due to the nonsymmetric electron density distribution on the Bi-O bond, which is enhanced by the substitution of neodymium ions for bismuth. As a result, the local inversion center in the dodecahedron vanishes. The displacement of oxygen ions leads to the variation of exchange coupling of Fe^{+2} -O-Fe^{+3}. The degeneracy of the t_{2g} states of Fe^{+2} ions is eliminated by the Bi^{+3} long pair and spin-orbit coupling. This leads to the change in the g factor of the ion and magnetic anisotropy. The electric field can be used to switch the magnetic anisotropy axis direction and the magnetic field, to switch the dipole moment direction via the spin-orbit coupling.

Thus, we describe the experimental data using the dipole glass model with the random orientation of dipole moments. This can be a cluster glass, which is realized in a system with competing anisotropies. In glass, there is a short-range order with a correlation length of 10 to 100 lattice constants with a random distribution of the anisotropy axes and the direction of the dipole moments. The modulus of the thermodynamic value of the dipole moment $|<P>|$ (an analog of the Edwards-Anderson parameter) is used as the order parameter, which vanishes in the vicinity of room temperature. The average polarization value is zero: $P = \sum_i p_i$, $p_i \neq 0$. The magnetic anisotropy is caused by the cubic symmetry of a crystal and additional contribution of the interface and surface effects. In a centrosymmetric crystal in magnetically ordered substances with several sublattices, an invariant in the form of a sum over various magnetic sublattices is possible:

$$f_{ME}^{lin} = -1/2 \sum_{ss'} \gamma_{ss'}^{ijk} P^i M_s^j M_{s'}^k \tag{2}$$

The energy dependent on the strain tensor and magnetic-field-dependent parameters can be presented as:

$$W = -\sum \beta_{kij} \varepsilon_k \sigma_i p_j - \sum \gamma_{ijk} p_i M_{Fe,j}^A M_{Fe,k}^B - \sum \alpha_{ij} M_{Fe,i}^A M_{Fe,j}^B \varepsilon_i - \sum G_{ij} \varepsilon_i M_{Rj} H_{ef,j} + \sum k\varepsilon_i^2/2 \tag{3}$$

where the first term describes the interaction between local dipole moments on the Bi–O bond and the elastic strain field, the second term describes the magnetoelectric interaction, the third term is related to the exchange variation upon straining or delocalization of electrons $\alpha = d\, J_{ij}\, (M_{Fe}{}^A\, M_{Fe}{}^B)/d\varepsilon$, and the fourth term is related to the interaction of the neodymium ion magnetic moment with the local exchange field of iron ion spins. In Eq. (3), $M_{Fe}{}^{B(A)}$ are the magnetic moments of iron ions, H_{ef} is the effective exchange field of iron ion spins on Nd^{+3}, and k is the elastic constant. The magnetostriction constant is determined in the form:

$$\lambda = d\varepsilon/dH = (\beta\sigma dP/dH + \alpha M_{Fe}^{A(B)} dM_{Fe}^{B(A)}/dH)/k + B(g\mu_B)^2 J(J+1) 2H_{ef}(dH_{ef}/dH)/(3\Delta k_B T) \tag{4}$$

The form of field and temperature dependences of the magnetostriction are caused by the polarization variation in a magnetic field at $T < T_d$ (T_d is the temperature of dipole glass formation) and magnetization in a magnetic field at $T < T_c = 450\,K$.

The film strain in an electric field can be determined from the relation:

$$\delta = d\varepsilon/dE = (\beta\sigma dP/dE + \alpha M_{Fe,i} dM_{Fe,j}/dE)/k) \tag{5}$$

It follows from Eqs. (4) and (5) that the temperature variations in the film strain in magnetic and electric fields in the dipole glass state will be similar. We calculate the film strain using the model of a superparamagnetic upon polarization variation in a magnetic (electric) field. In the low-temperature region, the polarization is directed along the anisotropy field. Upon heating, the anisotropy field rapidly decreases with increasing temperature, in contrast to the dipole moments, which tend to turn in the external field direction. As a result of the competition between the interaction of polarization with the anisotropy field and external magnetic (electric) field, the polarization grows and then decreases with increasing temperature. This can be described using the superparamagnetic model.

We express the energy of superparamagnetic particles as:

$$W = PH\cos\theta + PH_A\cos(\gamma - \theta) \tag{6}$$

where the angle θ specifies the electric polarization direction relative to the magnetic field, γ is the angle between the magnetic field and anisotropy field, and H_A is the anisotropy field. The equilibrium direction of the polarization is determined as $tg\theta = H_A \sin\gamma/(H + H_A\cos\gamma)$. We will present change of polarization in a magnetic field in the form:

$$\Delta P = P(\langle\cos\theta\rangle_H - \langle\cos\theta\rangle_0) = |<P>| \left(\sum_i \frac{1}{\sqrt{1 + \frac{H_A^2 \sin^2\gamma_i}{(H + H_A\cos\gamma_i)^2}}} - \frac{1}{\sqrt{1 + tg^2\gamma_i}} \right) = P_0(1 - T/T_d)^\beta \left(\sum_i \frac{1}{\sqrt{1 + \sin^2\gamma_i \Big/ \left[\frac{\mu}{(1 - T/T_d)^n} + \cos\gamma_i\right]^2}} - \frac{1}{\sqrt{1 + tg^2\gamma_i}} \right) \tag{7}$$

where $\mu = H/H_A$.

In the mean-field approximation, the modulus of the thermodynamic value of the dipole moment in the transition region is $|<P>| = P_0(1 - T/T_d)^\beta$ ($\beta = 0.35$). The anisotropy field also exhibits the power dependence $H_A = D\,(1 - T/T_d)^n$.

Above room temperature ($T > T_d$), the magnetostriction is caused by two competing contributions: the growth of magnetoelastic energy in a magnetic field at the transition to the magnetically ordered state below $T_c = 450\,K$ due to an increase in the volume and the single-ion mechanism related to the paraprocess of neodymium ion spins.

In the dipole glass state ($T < T_d$), the field dependences of magnetostriction of the films are determined by the polarization and magnetization variation in a magnetic field. Eq. (4) is reduced to the functional dependence:

$$\lambda = A_1 \Delta P/\Delta H + A_2 \Delta(M^2)/\Delta H + A_3/T\Delta(M^2)/\Delta H \tag{8}$$

The magnetic field suppresses temperature fluctuations of the magnetic moment and the Curie temperature increases in a magnetic field: $T_c(H) = T_c + \Delta T$. The temperature behavior of magnetization is described by the power function $M = M_0(1 - T/T_C)^\beta$.

$$\lambda = A_1 \Delta P/\Delta H + A_2[(1 - T/(T_c + \Delta T))^{2\beta} - (1 - T/T_c)^{2\beta}][1 - A_3/T] \tag{9}$$

The experimental data for the film on garnet are satisfactorily described by the following parameters: $\mu = 0.14$, $T_d = 250\,K$, $n = 2$, $\beta = 0.35$, $A_1 = 1.1 * 10^{-4}$, $A_2 = 0.01$, $T_c = 450\,K$, $\Delta T = 1\,K$, and $A_3 = 0.023\,eV$. For the film on glass, we have $T_d = 280\,K$, $\mu = 0.34$, $A_1 = 2.8 * 10^{-4}$, $A_2 = 0.022$, and $A_3 = 0.025\,eV$. In the $Nd_1Bi_2Fe_5O_{12}$(450 nm)/$Nd_2Bi_1Fe_4Ga_1O_{12}$(90 nm) film bilayer on glass, the piezoelectric interaction tensor and the exchange variation upon straining are twice as much as for the film on garnet.

The change in the film length in the electric field is determined by the rotation of dipole moments in the electric field direction $\Delta P/\Delta E$ and by the nonlinear electric-field dependence of magnetization $\Delta(M^2)/\Delta E$, which leads to the expansion of the film. The experimental electrostriction data are described by the functional dependence $\delta = A_1\, \Delta P/\Delta E - A_2\, E^n$, where exponent n decreases upon heating. The magnetostriction and electrostriction maxima are caused by rotation of electric (magnetic) moments along field as a result of the magnetoelectric interaction.

Above room temperature, when the state of dipole glass disappears, the field dependences of magnetostriction and electrostriction reveal a maximum. The positive value of the magnetostriction is due to the magnetoelastic interaction. The magnetic field suppresses the fluctuations of the magnetic moment, causes an increase in the correlation between the iron ions. The negative magnetoresistance is caused by the paraprocess of the magnetic moment of neodymium ions. There is also a nonlinear magnetoelectric effect quadratic in field, which gives a negative contribution to magnetostriction and with increasing temperature this contribution decreases.

4. Conclusions

The thermal expansion of the films is caused by two competing mechanisms: expansion of the films at the transition to the dipole glass state below room temperature and compression of the films caused by elastic stresses induced by the substrate. In the film on garnet, the elastic stress induced by the substrate prevails. The maximum film strain in the vicinity of the Curie temperature is related to the magnetoelastic interaction of iron ion magnetic moments.

Below room temperature, the films are compressed in magnetic and electric fields. We observed the magnetostriction anisotropy, change in its direction with temperature, and magnetostriction alternation in sign in the films on glass. The qualitative difference between the temperature behaviors of magnetostriction of yttrium neodymium and bismuth neodymium garnets was established. The magneto- and electrostriction maxima caused by the magnetoelectric interaction were found. These effects result from the change of the dipole (magnetic) moment direction under the action of the anisotropy field and external magnetic (electric) field. The alternation of magnetostriction in sign upon temperature variation is associated by competition of magnetoelastic interaction between iron spin and the paraprocess of neodymium ion spins.

Acknowledgement

This study were supported by the Russian Foundation for Basic Research project №18-52-00009 Bel_a, № 18-32-00079 mol_a, the state order № 3.5743.2017/6.7.

References

[1] H. Takagi, K. Takahashi, A. Tsuzuki, P. Lim, H. Uchida, M. Inoue, Preparation and fundamental properties of magneto-optic analog spatial light modulator with one dimensional magnetophotonic crystals, INTERMAG 2006 - IEEE Int. Magn. Conf. 2006, p. 241, , http://dx.doi.org/10.1109/INTMAG.2006.375823.

[2] T. Mizumoto, Y. Shoji, R. Takei, Direct wafer bonding and its application to waveguide optical isolators, Mater. (Basel). 5 (2012) 985–1004, http://dx.doi.org/10.3390/ma5050985.

[3] T. Ishibashi, Z. Kuang, S. Yufune, T. Kawata, M. Oda, T. Tani, Y. Iimura, K. Sato, Y. Konishi, K. Akahane, X. Zhao, T. Hasegawa, Magneto-optical imaging using polarization modulation method, J. Appl. Phys. 100 (2006) 93903, http://dx.doi.org/10.1063/1.2357699.

[4] S. Parchenko, A. Stupakiewicz, I. Yoshimine, T. Satoh, A. Maziewski, Wide frequencies range of spin excitations in a rare-earth Bi-doped iron garnet with a giant Faraday rotation, Appl. Phys. Lett. 103 (2013) 172402, http://dx.doi.org/10.1063/1.4826248.

[5] F. Atoneche, A.M. Kalashnikova, A.V. Kimel, A. Stupakiewicz, A. Maziewski, A. Kirilyuk, T. Rasing, Large ultrafast photoinduced magnetic anisotropy in a cobalt-substituted yttrium iron garnet, Phys. Rev. B – Condens. Matter Mater. Phys. 81 (2010), http://dx.doi.org/10.1103/PhysRevB.81.214440 214440.

[6] H. Kurebayashi, O. Dzyapko, V.E. Demidov, D. Fang, A.J. Ferguson, S.O. Demokritov, Controlled enhancement of spin-current emission by three-magnon splitting, Nat. Mater. 10 (2011) 660–664, http://dx.doi.org/10.1038/nmat3053.

[7] I.M. Syvorotka, S.B. Ubizskii, M. Kučera, M. Kuhn, Z. Vértesy, Growth and characterization of Bi, Pr- and Bi, Sc-substituted lutetium iron garnet films with planar magnetization for magneto-optic visualization, J. Phys. D. Appl. Phys. 34 (2001) 1178–1187, http://dx.doi.org/10.1088/0022-3727/34/8/308.

[8] L.E. Helseth, A.G. Solovyev, R.W. Hansen, E.I. Il'yashenko, M. Baziljevich, T.H. Johansen, Faraday rotation and sensitivity of (100) bismuth-substituted ferrite garnet films, Phys. Rev. B – Condens. Matter Mater. Phys. 66 (2002), http://dx.doi.org/10.1103/PhysRevB.66.064405 064405.

[9] N. Adachi, V.P. Denysenkov, S.I. Khartsev, A.M. Grishin, T. Okuda, Epitaxial Bi3Fe5O12(001) films grown by pulsed laser deposition and reactive ion beam sputtering techniques, J. Appl. Phys. 88 (2000) 2734–2739, http://dx.doi.org/10.1063/1.1287227.

[10] N. Adachi, T. Okuda, V.P. Denysenkov, A. Jalali-Roudsar, A.M. Grishin, Magnetic properties of single crystal film 1Bi3Fe5O12prepared onto Sm3(Sc, Ga)5O12(1 1 1), J. Magn. Magn. Mater. 242–245 (2002) 775–777, http://dx.doi.org/10.1016/S0304-8853(01)01007-1.

[11] Michimasa Sasakil, Gengjian Lou, Qi Liu, Minami Ninomiya, Takeshi Kato, Satoshi Iwata, Takayuki Ishibashi, Nd 0.5 Bi 2.5 Fe 5 − y Ga y O 12 thin films on Gd3Ga 5 O 12 substrates prepared by metal–organic decomposition, Jpn. J. Appl. Phys. 55 (2016), http://dx.doi.org/10.7567/JJAP.55.055501 055501.

[12] R.F. Al'muhametov, K.P. Belov, N.V. Volkova, Magnetic anisotropy of yttrium-neodymium garnet, Solid State Phys. 24 (1982) 1681–1684 https://inis.iaea.org/search/search.aspx?orig_q=RN:15042488.

[13] R.F. Al'muhametov, K.P. Belov, N.V. Volkova, Magnetostriction of yttrium - neodymium iron garnet ferrite, Solid State Phys. 25 (1983) 1499–1502 https://inis.iaea.org/search/search.aspx?orig_q=RN:15042488.

[14] Y.J. Wu, C. Yu, X.M. Chen, J. Li, Magnetic and magnetodielectric properties of Bi-substituted yttrium iron garnet ceramics, J Magn Magn Mater. 324 (2012) 3334–3337, http://dx.doi.org/10.1016/j.jmmm.2012.05.045.

[15] A.I. Popov, K.A. Zvezdin, Z.V. Gareeva, F.A. Mazhitova, R.M. Vakhitov, A.R. Yumaguzin, A.K. Zvezdin, Ferroelectricity of domain walls in rare earth iron garnet films, J. Phys. Condens. Matter. 28 (2016) 456004, http://dx.doi.org/10.1088/0953-8984/28/45/456004.

[16] A.P. Pyatakov, D.A. Sechin, A.S. Sergeev, A.V. Nikolaev, E.P. Nikolaeva, A.S. Logginov, A.K. Zvezdin, Magnetically switched electric polarity of domain walls in iron garnet films, EPL 93 (2011) 17001, http://dx.doi.org/10.1209/0295-5075/93/17001.

[17] Suleiman M. Elhamali, N.B. Ibrahim, S. Radiman, Structural, optical and magnetic properties of YIG doped with erbium and terbium nanofilms using sol-gel method, J. Adv. Nanomater. 1 (2016) 11002 https://dx.doi.org/10.22606/jan.2016.11002.

[18] N. Adachi, T. Okuda, V.P. Denysenkov, A. Jalali-Roudsar, A.M. Grishin, Magnetic properties of single crystal film $Bi_3Fe_5O_{12}$ prepared onto $Sm_3(Sc, Ga)_5O_{12}$ (1 1 1), J. Magn. Magn. Mater. 242–245 (2002) 01007–1011, http://dx.doi.org/10.1016/S0304-8853(01)01007-1.

[19] A.S. Sergeev, Mechanism of domain wall interaction with electric field in iron garnet films, J. Phys.: Conf. Ser. 929 (2017) 012085, http://dx.doi.org/10.1088/1742-6596/929/1/012085.

[20] E. Popova, A. Shengelaya, D. Daraselia, D. Japaridze, S. Cherifi-Hertel, L. Bocher, A. Gloter, O. Stéphan, Y. Dumont, N. Keller, Bismuth iron garnet Bi 3 Fe 5 O 12: A room temperature magnetoelectric material, Appl. Phys. Lett. 110 (2017) 142404, http://dx.doi.org/10.1063/1.4979826.

[21] B.B. Krichevsov, V.V. Pavlov, P.V. Pisarev, The giant linear magnetoelectric effect in garnet ferrite films, J. Exp. Theor. Phys. Lett. 49 (1989) 466–469 https://www.researchgate.net/publication/252544797.

[22] E. Kita, S. Takano, A. Tasaki, K. Siratori, K. Kohn, S. Kimura, Low-temperature phase of yttrium iron garnet (YIG) and its first-order magnetoelectric effect, J. Appl. Phys. 64 (1988) 5659–5661, http://dx.doi.org/10.1063/1.342262.

[23] Nobuyasu Adachii, Toshitaka Ota, Crystallinity and magnetic properties of Bi3Fe5O12 thick film prepared by MOD technique, J. Ceram. Soc. Jpn. 122 (2014) 40–43, http://dx.doi.org/10.2109/jcersj2.122.40.

[24] Y. Hosoe, R. Suzuki, K. Takanashi, H. Yasuoka, S. Chikazumi, Y. Sugita, NMR study of bismuth-substituted yttrium iron garnets, J. Phys. Soc. Jpn. 55 (1986) 731–734, http://dx.doi.org/10.1143/JPSJ.55.731.

[25] T. Oikawa, S. Suzuki, K. Nakao, First-principles study of spin-orbit interactions in bismuth iron garnet, J. Phys. Soc. Jpn. 74 (2005) 401–404, http://dx.doi.org/10.1143/JPSJ.74.401.

[26] S. Wittekoek, T.J.A. Popma, J.M. Robertson, P.F. Bongers, Magneto-optic spectra and the dielectric tensor elements of bismuth-substituted iron garnets at photon energies between 2.2-5.2 eV, Phys. Rev. B. 12 (1975) 2777–2788, http://dx.doi.org/10.1103/PhysRevB.12.2777.

[27] L.A. Bumagina, V.I. Krotov, B.Z. Malkin, A.Kh. Khasanov, Magnetostriction in ionic rare earth paramagnets, JETP 53 (1981) 792 http://jetp.ac.ru/cgi-bin/r/index/e/53/4/p792?a=list.